

Pressure measurements through image analysis

Sergio Calixto^{1*}, Francisco J. Sánchez-Marin¹, M. E. Sánchez-Morales²

¹ Centro de Investigaciones en Óptica, Loma del Bosque 115, Leon, Gto. C.p. 37150, MEXICO

² Centro Universitario La Cienega – U. de G., Universidad 1115, Col. Lindavista, Ocotlan, Jalisco, c.p. 47810 MEXICO

*scalixto@cio.mx

Abstract: Here we propose a new optical method, to our knowledge, to measure the pressure in liquids or gases by means of a flexible lens. Images of an object given by the dynamical lens are analyzed, and through the visibility of those images pressure is inferred.

©2009 Optical Society of America

OCIS codes: (120.0120) Instrumentation, measurement, and metrology; (100.2960) Image Analysis; (120.4640) Optical Instruments; (160.5470) Materials: Polymers; (160.4670) Materials: Optical Materials; (010, 1080) Adaptive Optics.

References and links

1. H. W. Babcock, "The possibility of compensating astronomical seeing," *Publ. Astron. Soc. Pac.* **65**, 229–236 (1953).
 2. N. Devaney, E. Dalimier, T. Farrell, D. Coburn, R. Mackey, D. Mackey, F. Laurent, E. Daly, and C. Dainty, "Correction of ocular and atmospheric wavefronts: a comparison of the performance of various deformable mirrors," *Appl. Opt.* **47**(35), 6550–6562 (2008).
 3. F. S. Tsai, S. H. Cho, Y. H. Lo, B. Vasko, and J. Vasko, "Miniaturized universal imaging device using fluidic lens," *Opt. Lett.* **33**(3), 291–293 (2008).
 4. S. Kuiper, and B. H. W. Hendriks, "Variable-focus liquid lens for miniature cameras," *Appl. Phys. Lett.* **85**(7), 1128–1130 (2004).
 5. J. Hardy, *Adaptive Optics for Astronomical Telescopes* (Oxford U. Press, 1998)
 6. D. Erickson, C. Yang, and D. Psaltis, "Optofluidics emerges from the laboratory," *Photonics Spectra* **42**, 74–79 (2008).
 7. G. Vdovin, and P. M. Sarro, "Flexible mirror micromachined in silicon," *Appl. Opt.* **34**(16), 2968–2972 (1995).
 8. S. Calixto, M. Rosete-Aguilar, D. Monzon-Hernandez, and V. P. Minkovich, "Capillary refractometer integrated in a microfluidic configuration," *Appl. Opt.* **47**(6), 843–848 (2008).
 9. H. Ren, and S.-T. Wu, "Variable-focus liquid lens," *Opt. Express* **15**(10), 5931–5936 (2007).
 10. K. Hosokawa, K. Hanada, and R. Maeda, "A polydimethylsiloxane (PDMS) deformable diffraction grating for monitoring of local pressure in microfluidic devices," *J. Micromech. Microeng.* **12**(301), 1–6 (2002).
 11. Y. Hongbin, Z. Guangya, C. F. Siong, and L. Feiwen, "Optofluidic variable aperture," *Opt. Lett.* **33**(6), 548–550 (2008).
 12. A. E. Vasdekis, G. E. Town, G. A. Turnbull, and I. D. W. Samuel, "Fluidic fibre dye lasers," *Opt. Express* **15**(7), 3962–3967 (2007).
 13. E. Borra, P. Hickson, and J. Surdej, "The International Liquid Mirror Telescope," *Optics and Photonics News* **20**(4), 28–33 (2009).
 14. S. Calixto, M. E. Sánchez-Morales, F. J. Sánchez-Marin, M. Rosete-Aguilar, A. M. Richa, and K. A. Barrera-Rivera, "Optofluidic variable focus lenses," *Appl. Opt.* **48**(12), 2308–2314 (2009).
 15. S. Calixto, F. J. Sanchez-Marin, and M. Rosete-Aguilar, "Pressure sensor with optofluidic configuration," *Appl. Opt.* **47**(35), 6580–6585 (2008).
 16. J. Xu, X. Wang, K. L. Cooper, and A. Wang, "Miniature all-silica fiber optic pressure and acoustic sensors," *Opt. Lett.* **30**(24), 3269–3271 (2005).
 17. X. Wang, J. Xu, Y. Zhu, K. L. Cooper, and A. Wang, "All-fused-silica miniature optical fiber tip pressure sensor," *Opt. Lett.* **31**(7), 885–887 (2006).
 18. M. Li, M. Wang, and H. Li, "Optical MEMS pressure sensor based on Fabry-Perot interferometry," *Opt. Express* **14**(4), 1497–1504 (2006).
 19. E. Cibula, S. Pevec, B. Lenardic, E. Pinet, and D. Donlagic, "Miniature all-glass robust pressure sensor," *Opt. Express* **17**(7), 5098–5106 (2009).
 20. D. Song, J. Zou, S. X. Wei, S. Yang, and H.-L. Cui, "High-Sensitivity fiber Bragg grating pressure sensor using metal bellows," *Opt. Eng.* **48**(3), 034403 (2009).
 21. <http://www.dowcorning.com/content/rubber/silicone-rubber.aspx>
 22. Federal Products Corporation, 1144 Eddy street, Providence Rhode Island 02940–9400 U.S.A.
 23. A. A. Michelson, *Studies in Optics* (The University of Chicago Press, 1968).
-

1. Introduction

Through time nature has developed and improved the mechanisms of living beings to better interact with their changing environment. Human eyes are dynamical organs because they can change their focal distances by a process known as accommodation. Although most of the power of the optical system of the eye is derived from refraction at the cornea, the changes in power during accommodation are effected by means of change in the shape of the crystalline lens. This change is controlled by the ciliary muscle.

Since ancient times, man has made optical elements with rigid and undeformable materials such as glass, crystals or metals. Among these elements were mirrors and lenses. Radius of curvature and refractive indexes of these passive elements remained fixed. About 50 years ago it was suggested that dynamical elements could be used for correction of atmospheric wavefronts [1]. At present dynamical elements are used for correcting ocular wavefronts [2], modification of laser beam profiles, in cellular telephones [3,4] and more. Those needs have given birth to the fields of adaptive optics [5] and optofluidics [6]. Adaptive optics mainly makes use of deformable mirrors which usually include a flexible membrane. The surface profile of such a mirror can be changed electrostatically [7]. Optofluidics elements are used in refractometers [8], variable-focus liquid lenses [9], deformable diffraction gratings [10], variable apertures [11], photonic crystal fluidic fiber lasers [12] and more [13]. Regarding variable-focus lenses, they can achieve their function by varying their refractive index [14] and/or by changing the curvature of their surfaces [15].

In the measurement of pressure, sensors with an electric output are commonly employed. However, like other electronic sensors, they are susceptible to electromagnetic interference (EMI) and changes in electrical conductivity. To avoid this electromagnetic interference optical methods have been proposed. They are based on the phenomena of interference of light (Fabry – Perot interferometer) [16–19], Fiber Bragg gratings [20] and microfluidic gratings [10], to mention but a few.

The sensor head of the detectors based on the Fabry – Perot structure can be made by MEMS technology using silicon [18] or by fabricating the resonant cavity in the tip of an optical fiber [16,17,19]. This method includes the splicing and cleaving operations. One surface of the cavity is a diaphragm that responds to pressure. It can be made of glass (fused silica), silicon or some polymer.

Methods based on fiber Bragg gratings rely on the axial stress of the grating made by pressure.

The method based on diffraction [10] can be implemented with a microfluidic diffraction grating. This grating consists of a series of rectangular grooves 5 μm wide by 2 μm depth, arrayed with a period of 10 μm . All the grooves are connected to a microchannel and their depths can be varied by applying pressure. If a light beam is sent to the grating this will be diffracted into several orders. Each one will have a given intensity. However, if pressure inside the grooves changes the intensity of the diffracted orders will also change. Therefore, pressure can be monitored by measuring the intensities of the diffracted beams. Here we present an optical method, as an alternative to electronic sensors, to measure pressure. The basis of this method is a deformable (flexible) lens that changes its focal length when pressure modifies the curvature of its surfaces. Due to this change in focal length images given by the lens also change. By analyzing the modifications in the image we can infer the pressure that affects the lens. This method is not based on diffraction as the one in reference 10.

This paper is organized as follows. In Section 2 is described the flexible lens fabrication method. Section 3 presents behavior of the focal length and profile of the lens surfaces as a function of the pressure applied to the lens. Section 4 shows the modifications that the image suffers when pressure is applied to the lens and the image analysis method through which pressure is inferred.

2. Lens fabrication method and cell layout

The material used to make the lens was silicone [21]. This material, besides being flexible, shows good transparency and stability with changes in humidity and

temperature. Additionally silicone copies perfectly the concavity and small features of glass surfaces. At the beginning of the lens fabrication process, a mixture of chemicals is prepared and poured between two glasses [14]. One of these glasses was a plane-parallel plate. The other had a concave surface. Then, glasses are left at rest for about 24 hours. After this time the oligomer is cured. At the end, glasses are separated and a plano-convex flexible lens is obtained, Fig. 1.



Fig. 1. A fabricated flexible lens

As mentioned above, deformable mirrors are used to correct atmospheric wavefronts. They do this by changing electrostatically its flexible membrane [7]. These changes are made locally. To change the whole profile of the fabricated flexible lens we have chosen to change the pressure of the medium that is in contact with one of its surfaces. Schematics of the cell used to perform this operation are shown in Fig. 2a. On one side of an acrylic cylinder a plane-parallel glass plate was glued. On the other side the plane surface of the lens was also glued, Fig. 2b. It should be noticed that the screw shown in the photograph had a central hole which let us increase or decrease the pressure inside the cell.

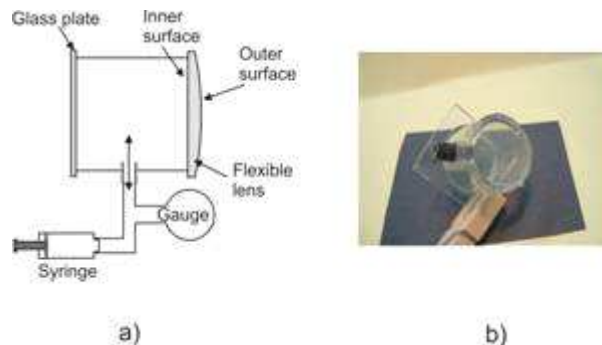


Fig. 2. a) Diagram of the cell used to change the pressure which in turn changed the curvature of the surfaces of the flexible lens. b) One of the fabricated cells. Notice the flexible lens. The screw has a hole in the center. Through it air was let to pass.

3. Lens characterization

The changes caused by pressure, to the profile of the inner and outer surfaces of the flexible lens, were assessed with a surface analyzer [22]. This instrument has a sharp needle that scans the surface under test. The result is a graph relating the height of the profile as a function of a linear coordinate.

The four upper curves of Fig. 3 represent profiles of the outer surface of a flexible lens. Each curve corresponds to a given pressure as indicated. As can be seen, as pressure increases the radius of curvature of the surface decreases.

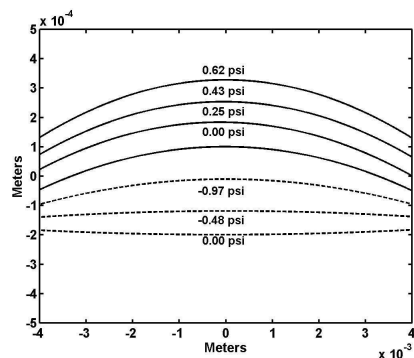


Fig. 3. Curves given by a surface analyzer of the surfaces of a flexible lens. Upper curves (continuous line) belong to the outer surface. Lower curves (dashed) belong to the inner surface. Parameter was the pressure in the cell. 1 psi = 6.89 KPa.

The inner surface of the lens was also studied when the lens was under pressure. However, because this surface was inside the cell the following equivalent method was used to study it: this time the convex side of the lens was glued to the edge of the acrylic cylinder. Then vacuum, instead of pressure, was applied by steps with the result that the plane surface of the lens began to bow. These results are also shown with the three dashed lines in Fig. 3. Notice that as pressure increases the profile of the inner lens surface passes from being close to a flat surface to a curve with a given radius. As pressure increases the radii of curvature diminishes. By viewing the graphs in Fig. 3 we can say that both lens surfaces suffer a modification and the lens becomes a meniscus.

To investigate the variation of the flexible lens focal length, as pressure inside the cell increases, the following experiment was done. A test target was placed about 4 m from the lens. Then with the help of a microscope the image of the target was located. Pressure in the chamber was increased, by steps, and the image position in every step was determined with the microscope. The behavior of the focal distance as a function of pressure in the cell can be seen in Fig. 4. It is possible to see that a linear relation is found.

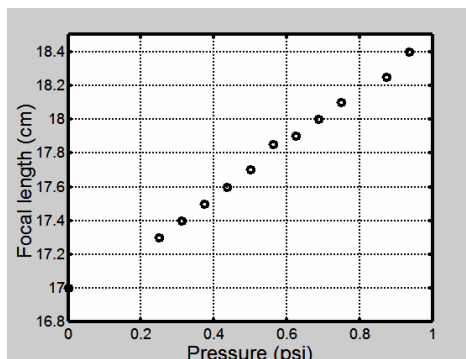


Fig. 4. Focal length as a function of the pressure in the cell.

The method outlined in the above paragraph could be used to find the pressure in the chamber. However, it is not practical because we need to find the image plane every time pressure is changed.

4. Image analysis and pressure measurements

The results given in this section were obtained with a prototype cell having a lens with a diameter of 2.5 cm and a focal length of 17 cm.

The method that we propose in this work, to measure the pressure in a cell, involves the modifications of an image formed by the lens in a given plane. Those modifications are due to the changes in focal distance by the applied pressure. Visibility of images is calculated and then it is related to pressure values. With these pairs of values, visibility

and pressure, a calibration graph is obtained. It should be noted that the visibility of images was evaluated in terms of the image contrast.

The object used in the measurements consisted of 4 vertical bars 2 mm wide. Space between bars was 1 mm. This object was placed about 2 m from the lens. The chamber pressure was increased by steps. Photographs in Fig. 5 show some of the images produced by the flexible lens when different pressures were applied. It should be noticed that when no pressure was present the edges of the bars were sharp. As pressure increased those edges became blurred.

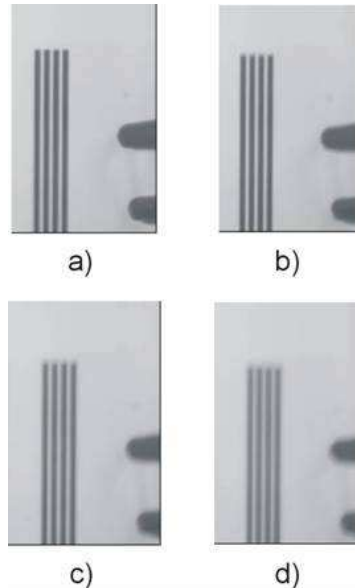


Fig. 5. Photographs of the images given by the flexible lens when different pressures were applied. a) 0 psi, b) 0.31 psi, c) 0.56 psi, d) 0.75 psi.

To calculate the visibility of the test images, a gray level profile of the images was obtained by averaging the gray level values of a five-pixel wide band (shown in black in Fig. 6a) and filtering the resulting one-pixel wide profile with a Gaussian filter in order to eliminate the remaining noise. The resulting profile was like the one shown in Fig. 6b.

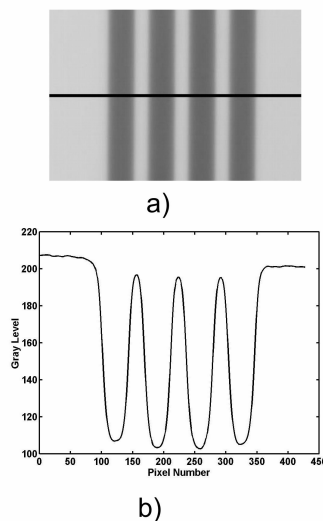


Fig. 6. a) Photograph of one image given by the flexible lens. A line with a width of 5 pixels has been drawn. b) Gray level vs. pixel number of the photograph in a).

By applying the method just described to a series of photographs, like the ones shown in Fig. 5, the profiles shown in Fig. 7 were obtained. Notice that as pressure increases valleys rise and maximum values decrease. One definition of visibility [23] is given by $V = (I_{\max} - I_{\min}) / (I_{\max} + I_{\min})$. By applying this definition to the profiles shown in Fig. 7 the visibility of the corresponding images can be assessed. Then it is possible to plot the visibility of the images as a function of the pressure in the chamber. This is shown in Fig. 8.

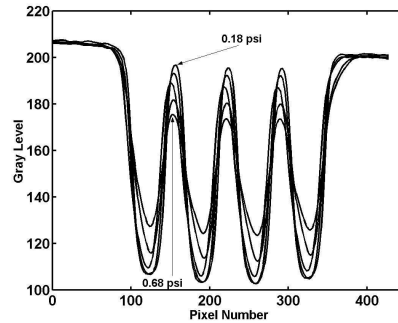


Fig. 7. Gray level as a function of pixel number

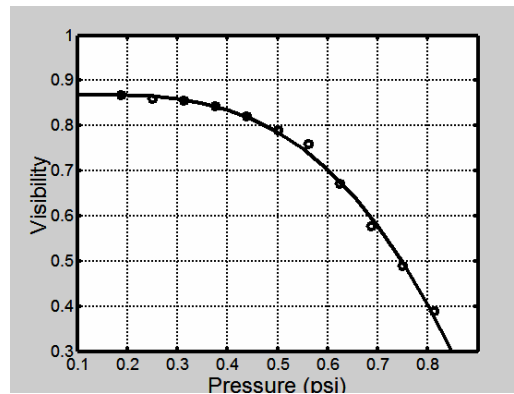


Fig. 8. Behavior of Visibility as a function of Pressure in the cell. Dots are experimental points. Continuous curve is an interpolated polynomial.

Commercial software was used to determine the polynomial that gave the best fit to the set of experimental measurements. The obtained formula was $v = 0.8683 - 0.0274 p + 0.4159 p^2 - 1.3843 p^3$. The curve that represents that polynomial was also plotted in Fig. 8. With that polynomial the value of an unknown pressure could be calculated once the visibility of the fringes has been determined.

5. Comments and Conclusions

We have shown an optical method to measure manometer pressure. This method relies on the deformation of a flexible lens by the applied pressure on its surface. Images given by the lens are analyzed and a calibration curve, in terms of the visibility of the images and pressure, is found.

The suggested method is versatile, can be automated, and can be adapted for different applications. The pressure range in which the prototype has been tested is between 0 psi and about 1 psi. However we foresee that this method can be applied in other ranges of pressure. To do this, configuration parameters can be changed. Among those parameters we have the curvature of the surfaces, the lens refractive index, and the stiffness and size of the lens. Lenses made with weak materials could respond faster to small changes in pressure. Stiff lenses could measure larger ranges. The size of the lenses could be adapted to fit in small locations. Curvatures of the flexible lens can be selected to get big or small images. Image size depends on the CCD sensor resolution.

Another parameter that can be selected is the material inside the cell. The results presented in this work were obtained when the cell was filled with air. However, we also investigated the behavior of the cell when it was filled with water; under this condition when pressure was applied focal length diminished. When water fills the cell the refraction at the interface between water - silicone is weak. This happens because the refractive index of water (1.333) and silicone (1.4126) are similar. Thus, the most important refraction occurs in the outer surface of the lens. As the curvature radius of that surface diminishes, while pressure grows, the lens focal distance also diminishes.

Although the methods mentioned in the Introduction section give good quality sensors, their fabrication and use require the use of expensive equipment; they incorporate multistep processes, increasing the probability of obtaining erroneous results. Besides they are sophisticated, time consuming, and involve health hazards.

The flexible lens method that we propose shows an acceptable precision is economical and the use of fewer and simpler pieces in the optical configuration means less trouble for a given application.

Acknowledgements

We thank fruitful discussions with Z. Malacara, Octavio Pompa, and people at the optical workshop of the Center for Research in Optics.